Gene Expression Profiling of Zebrafish Embryonic Retinal Pigment Epithelium In Vivo

Yuk Fai Leung,[1,2] *Ping Ma,*[2,3,4] *and John E. Dowling*[1]

Purpose. Eye development and photoreceptor maintenance is dependent on the retinal pigment epithelium (RPE), a thin layer of cells that underlies the neural retina. Despite its importance, development of RPE has not been studied by a genomic approach. In this study, a microarray expression-profiling methodology was established for studying RPE development.

Methods. The intact retina with RPE attached was dissected from developing embryos, and differentially expressed genes in RPE were inferred by comparing the dissected tissues with retinas without RPE, in microarray and statistical analyses.

Results. Of the probesets used, 8810 were significantly expressed in RPE at 52 hours postfertilization (hpf), of which 1443 may have biologically meaningful expression levels. Further, 78 and 988 probesets were found to be significantly over- or underexpressed in RPE, respectively, compared with retina. Also, 79.2% (38/48) of the known overexpressed probesets were independently validated as RPE-related transcripts.

Conclusions. The results strongly suggest that this methodology can obtain in vivo RPE–specific gene expression from the zebrafish embryos and identify novel RPE markers. (*Invest Ophthalmol Vis Sci.* 2007;48:881–890) DOI:10.1167/iovs.06-0723

The retinal pigment epithelium (RPE) is a thin monolayer of cells that underlies the retina and supports the function and development of photoreceptors.[1] A critical part of the visual cycle, the isomerization and oxidation of all-*trans*-retinol to 11-*cis*-retinal, takes place in the RPE. The 11-*cis*-retinal is transported back to the photoreceptor outer segment where it binds to the opsin protein to form rhodopsin.[2] The RPE is also important for the normal development of photoreceptor cells,[3,4] and it regulates the transport of various nutrients, ions and metabolic waste between the subretinal space and choroid, thus maintaining the proper physiological environment for the functioning of photoreceptors. Further, the RPE cells phagocytose and digest shed photoreceptor outer segment material. Dysfunction of the RPE is implicated in several eye diseases including retinitis pigmentosa (RP)[5] and age-related macular degeneration (AMD).[6] A better understanding of RPE development and physiology is important for characterizing its role in the pathophysiology of these diseases.

As yet, there have not been any genomic studies on RPE development. This is partly due to the difficulty in obtaining intact RPE tissue, as developing embryos are usually small. Most gene expression studies on RPE have been performed on cultured adult RPE cells[7–18] or dissected juvenile or adult RPE tissue.[19–26] Various genomic technologies including microarrays, RT-PCR, expressed sequence tag (EST) analysis, or serial analysis of gene expression (SAGE) have been used in these studies, which have provided important insights into the roles of the RPE in the pathophysiology of eye diseases. Among these studies, only the one by Dufour et al.[22] is the closest to a developmental study. They studied gene expression changes associated with photoreceptor outer segment phagocytic dysfunction in the RPE of the Royal College of Surgeons (RCS) rats at the age of 14 days, just after eyelid opening. However, at this stage, the retina has largely differentiated, and not much is known about the gene expression profile of developing RPE during early retinal development. Moreover, cells that are maintained in vitro may behave differently and have a different gene expression profile compared with their in vivo counterparts.[27–29] A study on in vivo RPE gene expression during development would assist in the understanding of the biology of the RPE.

Recently, we developed a methodology for microdissection of the intact retina from embryonic zebrafish[30] and have used this preparation for analyzing retinal gene expression at 36 and 52 hours postfertilization (hpf). The retinal microdissection technique we used destroys the RPE attached to the developing retina during removal. Nonetheless, it is technically feasible to keep the RPE cells attached to the retina during dissection and remove both tissues intact, thus providing the opportunity to subtract pure retinal expression data from this mixed tissue and obtain RPE-specific gene expression profiles by the appropriate statistical analysis.

Methods

Strain

Zebrafish were maintained according to standard procedures.[31] All procedures conformed to the ARVO Statement for the Use of Animals in Ophthalmic and Vision Research. The AB wild-type line was used in the study.

Dissection

Microdissection of zebrafish embryonic retina with RPE attached was performed based on a modified version of zebrafish embryonic retinal microdissection.[30] The embryos were collected at 10-minute intervals every hour, staged at 10 to 12 hours postfertilization (hpf) and restaged at 52 hpf, immediately before dissection. Two embryos were crushed completely in a 60 × 15-mm polystyrene culture plate (Falcon; BD Biosciences, Bedford, MA) containing Ringer's solution[31] to get rid of

From the [1]Department of Molecular and Cellular Biology, Harvard University, Cambridge, Massachusetts; and the [3]Department of Statistics, and the [4]Institute for Genomic Biology, University of Illinois, Champaign, Illinois.

[2]Contributed equally to the work and therefore should be considered equivalent authors.

Supported by a Fellowship from the Croucher Foundation and Knight's Templar Foundation (YFL), a grant from the Merck Award for Genomics Research (YFL, JED), a National Eye Institute Grant EY000811 (JED), and partially supported by a research grant from AstraZeneca and research board grant from University of Illinois (PM).

Submitted for publication June 28, 2006; revised September 13 and October 16, 2006; accepted December 18, 2006.

Disclosure: **Y.F. Leung**, None; **P. Ma**, AstraZeneca (F); **J.E. Dowling**, None

The publication costs of this article were defrayed in part by page charge payment. This article must therefore be marked "*advertisement*" in accordance with 18 U.S.C. §1734 solely to indicate this fact.

Corresponding author: Yuk Fai Leung, Department of Molecular and Cellular Biology, Harvard University, 16 Divinity Avenue, Cambridge, MA, 02138; yfleung@mcb.harvard.edu.

the adhesiveness of the culture plate surface 30 minutes before dissection. The head with part of the anterior trunk was cut off from the body and the brain removed, as described previously.[30] In contrast to the retinal dissection, the RPE was not brushed away. Rather, the eye tissue was lifted gently from the posterior lateral side by a Dumont 55 forceps tip (World Precision Instruments, Sarasota, FL) and rolled to the anterior side (Figs. 1A, 1B). During the process, the lens was removed with a chemically etched tungsten needle (Fig. 1C). The presumptive choroid and scleral tissue on the outside of the RPE layer was attached relatively tightly to the skin and was mostly peeled off by rolling the eye carefully to the anterior side (Figs. 1C–E). Ten such tissues were pooled as one biological replicate, and three independent replicates were collected.

Histology

The whole embryo, dissected retina, and retina with RPE attached were fixed overnight in a solution of 4% paraformaldehyde in phosphate-buffered saline (PBS) at 4°C. They were washed three times for 5 minutes each in PBS with 0.1% Tween-20 (PBST) at room temperature. The samples were dehydrated through an ethanol series (50%, 70%, 85%, 90%, and 95% and two times at 100% [vol/vol]) ethanol) for 10 minutes in each. Infiltration of epoxy resin was achieved by washing the samples in propylene oxide (Electron Microscopy Sciences, Hatfield, PA) twice for 15 minutes each; in equal parts of propylene oxide and Epon/Araldite resin (Electron Microscopy Sciences) for 2 hours; and in one part of propylene oxide and three parts Epon/Araldite with caps open overnight to allow for propylene oxide evaporation and resin infiltration for overnight. The samples were embedded in pure Epon/Araldite resin, and incubated at 60°C for 2 days until the resin hardened. One-micrometer-thick sections were cut, mounted on gelatin-coated slides, and stained with a mixture of 1% azure II and 1% methylene blue in an aqueous 1% borax solution. The sections were mounted on slides using chemical mountant (DPX; Electron Microscopy Sciences) and imaged by a digital camera (Retiga Exi; QImaging, Burnaby, BC, Canada) on a fluorescence microscope (DMRB; Leica, Deerfield, IL), and the images were subsequently processed (Photoshop ver. 6.0; Adobe Systems Inc., Mountain View, CA).

Total RNA Extraction and Microarray Experiment

Total RNA extraction was performed by combining TRIzol (Invitrogen, Carlsbad, CA) and a column-based extraction procedure (Qiagen, Valencia, CA) with modifications, as described previously.[30] The yield and purity of the extracted RNAs were evaluated by measuring the ultraviolet (UV) absorbance in a spectrophotometer (NanoDrop Technologies, Rockland, DE) and electrophoresing one microliter of the sample (RNA 6000 Nano LabChip running in a 2100 Bioanalyzer; Agilent Technologies, Palo Alto, CA). Thirty-three nanograms of the total RNAs extracted from retinal, and RPE attached retinal samples were amplified and labeled using a two-cycle target-labeling protocol (Affymetrix, Santa Clara, CA), and hybridized to whole genome microarrays (GeneChip Zebrafish Whole Genome Arrays; Affymetrix). All hybridization, washing, and scanning were performed according to the manufacturer's standard procedure.

Data Analysis

The probe-level data were background adjusted, normalized, and summarized by a robust multiarray average (RMA) algorithm[32] implemented in the software package affy of the Bioconductor project, release 1.7 (http://www.bioconductor.org/ available in the public domain and based at the Fred Hutchinson Cancer Research Center, Seattle, WA), running in the R statistical environment, version 2.2.0 (http://www.r-project.org/ available in the public domain and hosted by the Department of Statistics and Mathematics, Wirtschafts Universität, Vienna, Austria), using default parameters.

The starting total RNA amount for the array experiments was standardized to 33 ng. However, the retina with RPE attached at 52 hpf (WRR52) samples actually contained both RPE and retinal tissues (compare Figs. 2E, 2F). In theory, the retinal contribution in the WRR52 gene expression should be the same as in pure retina at 52 hpf (WR52). Therefore, WR52 expression levels were used to estimate this retinal contribution and assist in the calculation of the RPE contribution at 52 hpf (RPE52). First, the WRR52 expression levels were adjusted by the ratio of total RNA yield of WRR52 to that of WR52 as follows:

$$\text{adjExprWRR52}_{ij} = \text{ExprWRR52}_{ij} \times \frac{\overline{\text{YieldWRR52}}}{\overline{\text{YieldWR52}}}, \quad i = 1, \ldots, n, \quad j = 1, 2, 3 \quad (1)$$

where adjExprWRR52_{ij} and ExprWRR52_{ij} are the adjusted and (unadjusted) WRR52 expressions of gene i in jth replicate, respectively, and $\overline{\text{YieldWRR52}}$ and $\overline{\text{YieldWR52}}$ are the sample averaged RNA yields of WRR52 and WR52, respectively, in the three biological replicates. Because the sample size was small in this study (only three replicates), the sample mean was used to estimate the true mean yield.[33] A nice property of the sample mean is that it is close to the true mean yield on average, which is an unbiased estimator, no matter what the distribution of the sample is. As the sample size increases, the probability that the sample mean will fall outside the small neighborhood of the true mean is negligible. In other words, the sample mean is an efficient estimator of the true mean. In this study, the yields of the three biological replicates of WRR52 and WR52 were 218.69, 179.83, and 266.87, and 170.1, 179.93, and 153.22 ng, respectively.

Assuming that the expression levels are normally distributed and the adjusted WRR52 expression contains both the WR52 expression and RPE expression—that is, $\text{adjExprWRR52}_{ij} \sim N(\theta_{1i}, \sigma^2_{1j})$ and $\text{ExprWR52}_{ij} \sim N(\theta_{2i}, \sigma^2_{2j})$, where $\theta_{1i} = \theta_{2i} + \theta_{0i}$ and θ_{0i} are the true RPE expression levels of gene i, then the true RPE expression θ_{0i} was estimated by

$$\hat{\theta}_{0i} = \overline{\text{adjExprWRR52}}_i - \overline{\text{ExprWR52}}_i, \quad i = 1, \ldots, n, \quad (2)$$

where $\hat{\theta}_{0i}$ is the estimated true RPE52 expression level of gene i and $\overline{\text{adjExprWRR52}}_i$ and $\overline{\text{ExprWR52}}_i$ are the sample means of adjusted WRR52 and (unadjusted) WR52 expression levels in the three biological replicates. In some cases, the estimates were negative, and their values were truncated to zero.[34]

The $100(1 - \alpha)\%$ confidence interval of the true RPE52 expression levels of gene i was constructed as

$$\hat{\theta}_{0i} - t_{\alpha/2}\sqrt{\frac{S^2_{1i}}{3} + \frac{S^2_{2i}}{3}}, \quad i = 1, \ldots, n, \quad (3)$$

where $t_{\alpha/2}$ is $100(1-\alpha/2)$ percentile of Student's t distribution with four degrees of freedom, S^2_{1i} and S^2_{2i} are sample variance of adjusted and (unadjusted) WRR52 expression level of gene i.

A gene was inferred as significantly expressed in RPE52 if the corresponding lower 90% confidence limit of the estimate was greater than 0—that is, with 90% confidence there is an expression of the gene that is greater than background (i.e., 0). An arbitrary cutoff of a 90% lower bound of the RPE52 estimate $\geq$41.87 was used to select genes that might be biologically meaningful (see the Results section). A gene was deemed not expressed in RPE52 if the corresponding lower 90% confidence limit of the estimate was $\leq$0.

A fold change between expression of RPE52 and that of WR52 was defined as

$$\frac{\theta_{0i}}{\theta_{2i}} = \frac{\theta_{1i}}{\theta_{2i}} - 1. \quad (4)$$

Let $r_i = \frac{\theta_{1i}}{\theta_{2i}}$; then, the inference on r_i can be based on a pivotal quantity

$$Q_i = \frac{(\overline{\text{adjExprWRR52}_i} - r_i \times \overline{\text{ExprWR52}_i})^2}{\sigma_{1i}^2/3 + r_i^2 \times \sigma_{2i}^2/3},$$

which has a χ^2 distribution with 1 *df*. Thus, a confidence interval based on Q_i, can be constructed for r_i if S_{1i}^2 and S_{2i}^2 are substituted for σ_{1i}^2 and σ_{2i}^2.[34,35] Then 1 was subtracted from r_i to obtain the confidence interval for the fold change $\frac{\theta_{0i}}{\theta_{2i}}$. The calculation was conducted using dChip (http://www.dchip.org/ developed in a collaborative effort and available in the public domain). Because the expression change should be nonnegative, the resultant negative estimates were truncated to zero. A lower 90% confidence limit of RPE52/WR52 >1 was used to infer significant overexpression, and a higher 90% confidence limit of RPE52/WR52 <1 was used to infer significant underexpression of the genes, with the lower bound of the RPE52 estimate at ≥41.87.

All gene annotations were adopted from an annotation file prepared by Affymetrix on December 19, 2005. The overexpressed genes with only a clone ID or a locus number were further analyzed by searching the Affymetrix Probeset ID in the Ensembl database (http://www.ensembl.org/; version Zv5, May 2005; provided in the public domain by The Ensembl Genome Database Project), and the title and the symbol of the corresponding human homologues were retrieved if available. The whole dataset is available at the Gene Expression Omnibus (http://www.ncbi.nlm.nih.gov/projects/geo/ provided in the public domain by the National Center for Biotechnology Information, Bethesda, MD) under the accession number GSE5048.

Results

The retina with RPE attached at 52 hpf (WRR52) was dissected as described in Figure 1 and the Methods section. The reason for choosing 52 hpf for the study is that the photoreceptors are just beginning to differentiate at this stage,[36] which roughly corresponds to postnatal day (P)8/9 in rats[37] and mice,[38] when rhodopsin and photoreceptor outer segments begin to form. There is substantial evidence that the developing RPE plays important roles in photoreceptor development.[3,4] The candidate genes identified at this stage may thus provide further insights into these roles. Most of the presumptive choroid and scleral tissue outside the eye can be successfully removed without affecting RPE integrity, as shown by gross morphology (Figs. 2A, 2B) and histology (Figs. 2D, 2E). The dissection methodology for obtaining the developing retina intact from embryonic zebrafish has been described previously.[30] This method removes virtually all RPE from the retina (Fig. 2C) without compromising the integrity of the extracellular matrix between the presumptive photoreceptor layer and the RPE (Fig. 2F, arrowhead).

The gene expression levels of three independent replicates of WRR52 tissue, consisting of 10 samples each, were measured by the microarray expression profiling methodology, as described previously, and compared with the microarray expression data from three independent WR52 samples obtained from an ongoing genomic study on retinal development in zebrafish (Leung et al., unpublished data, 2006).

The pair-wise correlation coefficients of the Perfect-Match (PM) probes from the microarray results among the three biological replicates suggest that our methodology can give highly reproducible gene expression measurements. The correlation coefficients of the three WRR52 biological replicates were 0.9904, 0.9925, and 0.9905. These are slightly higher than those for WR52, which were 0.9756, 0.9785, and 0.9811. This difference probably occurred because the three WRR52 replicates were processed in parallel, whereas the three WR52 replicates were processed independently. The retinal dissection may also cause some retinal damage in the WR52 samples during the RPE removal step, resulting in a slightly higher variation in the expression measurements. Nonetheless, the correlation coefficients are very high, indicating that the method is consistent and not substantially affected by experimental errors.

The starting total RNA amount for the microarray labeling protocol was standardized to 33 ng. If the resultant expression measurements of the WRR52 and WR52 samples from the arrays were compared with each other directly, it would be equivalent to assuming that the two types of samples give equal amounts of total RNA. However, the total RNA yield of the WRR52 samples should be slightly higher than the WR52 samples, as they contain additional total RNAs from the RPE cells. Therefore, the yields of the WRR52 samples were used to adjust the expression levels (equation 1). The WR52 expression levels were assumed to be equivalent to the retinal contribution in the adjusted WRR52 samples and deducted from the WRR52 expression levels to obtain estimations of RPE gene expression at 52 hpf (RPE52; equation 2).

There were 8810 probesets shown to have a significant expression above zero in the RPE52 estimates (90% lower bound RPE52 estimate >0; Table 1 and Supplementary Table S1, online at http://www.iovs.org/cgi/content/full/48/2/881/DC1). Among these probesets, 1443 have a lower bound RPE52 estimate of at least 41.87, which is likely to be biologically meaningful, as one of the overexpressed genes, *anxa2a*, known to be present in the RPE, has the lowest expression estimate (41.87) of all the genes that have been experimentally validated (discussed later).

A final fold change was calculated using these RPE52 estimates and their corresponding WR52 expressions (equation 4). Seventy-eight probesets were found to be overexpressed in RPE when compared with the retina at 52 hpf (90% lower bound of RPE52/WR52 fold change >1; Tables 1, 2). Twenty-seven of them have annotations (i.e., with names), and the human homologues of 21 additional probesets with only a clone or locus number were retrieved from the Ensembl database (Table 2). Several of these are melanoblast and neural crest (which gives rise to pigment cells) markers, including *dct*,[39] *gch*,[40,41] and *crestin.*[42] *Rab32*, *pah* (an enzyme that converts phenylalanine to tyrosine and is involved in melanin production[43]), *col9a2*, and *nme4* have a specific expression in the RPE layer at the similar developmental long-pec stage, as shown by in situ hybridization data available in the ZFIN (Zebrafish Information Network) database (http://zfin.org).[44,45] *RPE65*[46] and *RGR*[47] are RPE-specific genes, and *AQP1* has been identified in RPE and implicated in transepithelial water transport.[48] *Lamb1* has been isolated from a retinal blowout mutant in a recent large-scale insertional mutant characterization study.[49] The retina in this mutant is expelled through the RPE into the forebrain, suggesting that *lamb1* may be involved in maintaining RPE integrity. *Gart* is a mutant that has been isolated in a sister insertional mutagenesis screen[50] and has spotty pigment in the RPE and small eyes (ZFIN ID: ZDB-FISH-050,809-9). *Tagln2* has been identified from SAGE[19] and microarray studies[12] on RPE biopsy specimens and cultured RPE cells, respectively. Of note, it is also differentially expressed in human embryonic stem cell-derived RPE cells that are transdifferentiated into neural progenitors, which highly resemble human embryonic stem cells,[51] suggesting that the RPE at 52 hpf in zebrafish may still not be fully differentiated. *Col2a1a* has been shown to be expressed in the outer layer of the optic cup, the precursor of the future pigment layer of the retina in E11.5 mouse embryos.[52] Annexin A2, the protein product of *anxa2a*, has been shown to be expressed in the apical microvilli of the mouse RPE by proteomic analysis.[53] In another proteomic study, HSP70, the protein product of *HSP70*, has been found to be downregu-

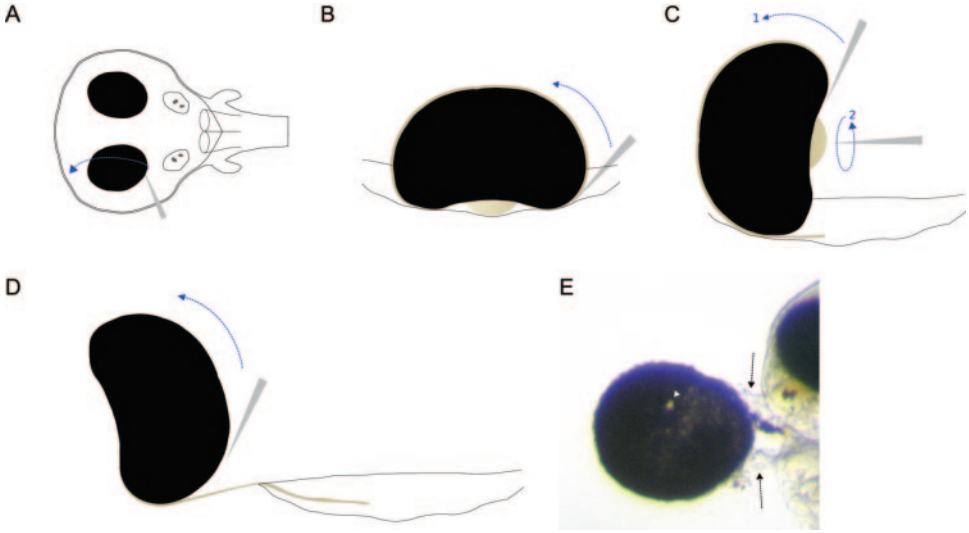

FIGURE 1. Dissection procedures for retina with RPE attached at 52 hpf (WRR52). (**A**) Dorsal view of the opened head. The head is cut open and the brain removed as previously described.[30] The WRR52 is dissected by gently rolling the whole eye from the posterior side (*right* in the diagrams) to the anterior side (*left* in the diagrams). The medial side of the eyes is facing upward after flattening the opened head. (**B**) The side view of (**A**). (**C**) The lens is removed during the rolling process by a tungsten needle with a swirling motion. (**D**) Removal of the presumptive choroid and scleral cells. These tissues preferentially stick to the remnant of the skin during the rolling process and are removed from the WRR52. (**E**) An image of a partially dissected WRR52. *Black arrows*: presumptive choroid and scleral cells; *white arrowhead*: optic nerve. There is usually at least one melanocyte in the presumptive choroid and scleral region (the dark patch in the partially removed tissue).

lated in the RPE of patients with early-stage AMD.[54] *ACSL1*, *AHNAK*, *arfip1*, *arr3l* (human orthologue: *ARR3)*, *ATIC*, *cd63*, *col9a2*, *eno3*, *FHL3*, *GLB1L*, *gpd1l*, *gstp1*, *hsp47* (human orthologue: *SERPINH1*), *krt8*, *krt18*, *runx2a* (human orthologue: *RUNX2*), *TMED3*, *TNFRSF10B*, and *TPD52* have been identified in an un-normalized human RPE/choroid EST library,[21] whereas *Tuba8l3* has been identified in a zebrafish posterior segment/rpe/choroid EST library (NEIBank: NbLib0095). There is a duplicated probeset for *krt18*, *hsp70*, *PMP22*, and *RPE65*. There is currently no other information about the relationship of the remaining probesets (*cpn1*, *KRT13*, *MB*, *mpx*, *MRPS18B*, *PHLDA2*, *PMP22* [two probesets], *RAD9A*, and *TSSC1*) and RPE, suggesting that they may be potential RPE markers. In short, 79.2% (38/48) of the known probesets have been independently validated as RPE-related transcripts. Since many significant probesets are still unannotated genes or ESTs, it is likely that they represent additional novel RPE-specific markers.

Six thousand six hundred ninety-two probesets had a lower bound RPE52 estimate of less than 0 and were deemed not to be expressed in RPE52 (Table 1 and Supplementary Table S2 http://www.iovs.org/cgi/content/full/48/2/881/DC1). Also, 988 of the 1443 probesets with the lower bound RPE52 estimate of at least 41.87 were found to be underexpressed in RPE (i.e., upper bound of RPE52/WR52 fold change <1; Table 1 and Supplementary Table S3). For example, several cell cycle genes were either not expressed or were underexpressed in RPE (not expressed: *ccna1*, *ccnd1*, *ccne*, *ccnf*, *ccng1*, *ccng2*, *ccni*, *cdk2*, and *cdk8*; underexpressed: *ccna2*, *ccnb1*, *ccnb2*, *ccng2*, *cdc2*, and *cdc20*), suggesting that RPE cells at 52 hpf are more differentiated than the retinal cells and hence show a suppression of the genes for proliferation. *Cdh2* and *cdh4* are neural- and retina-specific adhesion molecules[55] that were not expressed in RPE52. *Alcam*[56] and *Atoh7/ath5*[57], a zn-5/zn-8 antigen which labels retinal ganglion cells (RGC) and a gene that specifies the RGC fate, were also not expressed

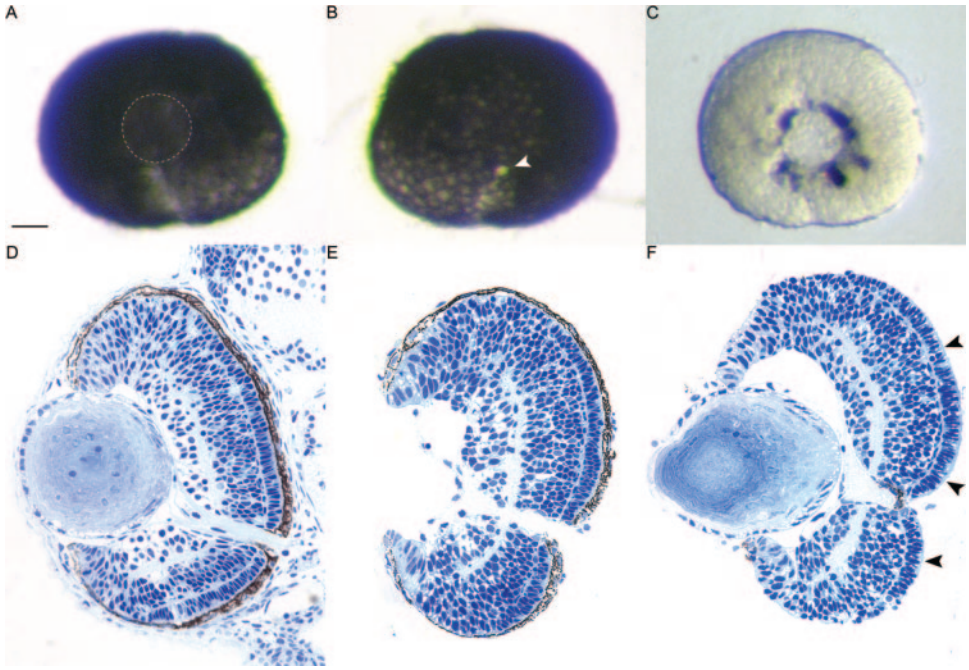

FIGURE 2. (**A**) A WRR52 sample, lateral view. This particular sample is the left eye of the embryo. The area encircled by the *dotted line* is the lens cavity. Anterior is to the *left,* dorsal is *up.* (**B**) The WRR52 sample in medial view. Note that there are no RPE cells in the region where the optic nerve leaves the retina (*arrowhead*). Anterior is to the *right*, dorsal is *up*. (**C**) A WR52 sample. The orientation is the same as in (**A**). Histologic sections of the retina from a whole embryo (**D**), WRR52 (**E**), and WR52 (**F**). Note that the extracellular matrix between the presumptive photoreceptor layer and the RPE remains intact after retinal dissection (**F**, *arrowheads*), suggesting that mechanical damage is minimal. Scale bar, 50 μm.

TABLE 1. A Summary of the Number of Significant Genes Selected by Different Criteria

Category	Selection Criteria	Selected Genes (*n*)
Genes expressed in RPE at 52 hpf	90% lower bound of RPE estimate >0	8810
Genes expressed in RPE at 52 hpf, biologically more relevant	90% lower bound of RPE estimate >41.87	1443
Genes not expressed in RPE at 52 hpf	90% lower bound of RPE estimate ≤0	6692
Genes differentially over-expressed in RPE compared to retina at 52 hpf	90% lower bound of RPE52/WR52 change >1-fold	78
Genes differentially under-expressed in RPE compared to retina at 52 hpf	90% lower bound of RPE estimate >41.87 and 90% upper bound of RPE52/WR52 change < 1-fold	988

in RPE52. Further, several genes implicated in synaptogenesis, photoreceptor structure, and visual signal transduction and that are not expressed in RPE were not or were underexpressed in RPE52 samples (not expressed: *gria2.1*, *ctbp2*, *gc2*, *gpr19*, *gnat1*, *gngt2*, *syap1*, *syncripl*, *sypl*, and *syt4;* underexpressed: *ift52*, *ift57*, *rims2*, *syt11*, and *tbl2*).

DISCUSSION

We have successfully developed a methodology for microdissecting and estimating gene expression levels in developing zebrafish RPE in vivo. The dissection quality is high, and the resultant total RNAs from the tissues yield consistent and reproducible gene expression levels. About 80% of the known significant genes have been experimentally validated to be related to or are specific to the RPE. This strongly suggests that the statistical analysis has separated the genes that are truly overexpressed from those that are not expressed or are underexpressed in RPE and has identified several possible novel RPE developmental markers.

The present profiling approach complements other techniques including EST and SAGE screening, because it is much more flexible and scalable. It does not require much starting RNA and can easily incorporate additional time points. The identified candidate genes can be functionally validated relatively easily by harnessing existing experimental approaches for the zebrafish model, including in situ hybridization and antisense morpholino gene knockdown. The retinal dissection methodology has been characterized in 36- and 52-hpf embryos and successfully performed on 24-hpf embryos and 3-day postfertilization (dpf) larvae.[30] Because the retinal dissection is technically more demanding than the dissection of retina with RPE attached, the present methodology can be extended to other time points as well. Furthermore, these stages cover important eye developmental events in zebrafish: (1) Early proliferation and growth of the retina (24 hpf); (2) differentiation of the first neuronal cell type–retinal ganglion cells (36 hpf)[36]; (3) differentiation of the first photoreceptor cells and formation of neuronal connections within the retina (retinal lamination; 52 hpf)[36]; and (4) the first visual responses that indicate the retina has developed to a functional state (3 dpf).[58,59] As a result, the RPE expression-profiling methodology has opened the possibility of studying gene expression of developing RPE concurrently with retina for the first time and provides the opportunity for further understanding of the genetic interactions between the two tissues during critical developmental stages. In particular, the candidate genes identified in the present study could provide further information on the role of RPE in early photoreceptor differentiation.

A major limitation of this methodology is that it measures the average expression in all the RPE cells, essentially treating them as a homogeneous tissue. This is not an accurate assumption for most developing tissues, in which different morphogenic gene signals and gradients operate together to form the tissue. In zebrafish eye development, it is well known that the initial differentiation of different neural layers in the retina is controlled by several neurogenic waves, which start from the ventronasal retina, spread through the dorsal retina in a circular sweep, and finally reach the ventrotemporal retina.[36,60,61] It is very likely that RPE development is also subject to neurogenic wave regulation and has a spatial expression difference. There are at least two bits of evidence that support this hypothesis. Stenkamp et al.[4] have found that sonic hedghog (*shh*) and tiggy-winkle hedgehog (*twhh*) have a discrete expression pattern from anterior to posterior RPE in 54-hpf embryos, and this expression is in advance of photoreceptor differentiation. It has also been demonstrated that *shh* and *twhh* functions are important for the progression of rod and cone photoreceptor differentiation. In the present study, we also observed a morphologic difference in the RPE in the same eye at 52 hpf. Figure 2B shows the RPE in the ventrotemporal area (lower left corner of the sample) is paler than the RPE on the nasal side (right on the diagram), and the RPE nuclei (the whiter patches) are much more apparent in the ventrotemporal region. These observations suggest that melanin production in the ventrotemporal RPE is less extensive than on the nasal side and that the cells in the RPE layer are at different stages of differentiation. As a result, one has to take into account the potential spatial regulation of the candidate genes identified by this approach and validate the spatial expression pattern by in situ hybridization before making any functional interpretations.

Two assumptions were made during the analysis to estimate RPE52 expression: (1) The total RNA yields can be used as a reference to adjust the expression levels; and (2) the WRR52 expression is the sum of WR52 and RPE52 expression. In principle, these assumptions are valid. However, the total RNA yields can be subject to experimental variations that can lead to biased estimates of RPE52 expression and, in turn, the corresponding fold change calculations. Thus, imposing a cutoff on the change alone may not be adequate to identify differentially expressed RPE genes. Therefore, a 90% confidence interval was used instead of 95%, to tolerate the potential bias.

It is also possible to estimate RPE expression levels at 52 hpf and the associated fold changes compared with the retina by an alternative approach based on a weighted-average assumption (Supplementary File, online at http://www.iovs.org/cgi/content/full/48/2/881/DC1). This approach further adjusts the RPE52 and WR52 expression estimates by their yields before calculating the changes. Whereas the onefold cutoff threshold becomes approximately threefold in the alternative approach, the resultant number of significantly expressed genes in RPE at 52 hpf, as well as the ranking of the fold changes between the RPE and retina remain the same. In theory, one can further lower the cutoff threshold in this approach and obtain more potential RPE-specific candidate genes. For example, if a onefold cutoff threshold is used to infer significance, 1878 genes will be inferred as significantly overexpressed, and 1700 genes with change >0-fold will be inferred as significantly underexpressed in RPE when compared with retina at 52 hpf.

TABLE 2. Seventy-Eight Overexpressed Genes in the RPE Compared with the Retina at 52 hpf

Probe Set ID	Gene Name	Gene Symbol	Adjusted WRR52 Mean Expression	RPE52 Estimate	WR52 Mean Expression	Fold Change of RPE52/WR52	90% Lower Limit of RPE52/WR52	90% Upper Limit of RPE52/WR52
Dr.12451.2.A1_at	zgc:73213; Retinal pigment epithelium-specific protein 65kDa*‡	zgc:73213; *RPE65**‡	1114.39	1040.59	73.79	14.1	9.16	19.8
Dr.24891.1.S1_at	Hypothetical protein LOC568958	LOC568958	738.5	669.91	68.6	9.77	5.44	20.24
Dr.11274.1.A1_at	Similar to melanosomal matrix protein precursor	LOC563293	507.92	455.03	52.9	8.6	4.41	13.05
Dr.14668.1.S1_at	GTP cyclohydrolase 1*	*gch**	285.83	255.39	30.44	8.39	4.23	13.27
Dr.16101.1.S1_at	—	—	635.32	562.52	72.8	7.73	4.79	12.46
Dr.10336.1.S1_at	Dopachrome tautomerase*	*dct**	1488.51	1299.37	189.14	6.87	4.62	9.2
Dr.8124.1.S1_at	Crestin*	crestin*	429.13	354.37	74.76	4.74	3.73	5.79
Dr.14747.1.A1_at	zgc:113085	zgc:113085	175.79	143.39	32.41	4.42	3.56	5.29
Dr.5258.1.A1_at	wu:fc51h06	wu:fc51h06	192.78	156.92	35.87	4.38	2.72	6.25
Dr.4884.1.S1_at	zgc:109930; Retinal G protein coupled receptor*‡	zgc:109930; *RGR**‡	747.96	600.77	147.19	4.08	2.66	5.57
Dr.9225.1.A1_at	—	—	115.11	91.57	23.54	3.89	3.19	4.6
Dr.3761.1.S1_at	Collagen type II, alpha-1a* /// similar to collagen alpha 1(II) chain precursor-bovine (tentative sequence) (fragments) /// similar to collagen II A1	*col2a1a** /// LOC562496 /// LOC564438	283.29	223.35	59.94	3.73	1.42	6.04
Dr.1282.1.S1_at	Keratin 8*	*krt8**	207.72	161.64	46.08	3.51	2.61	4.55
Dr.14035.2.A1_at	Similar to cornifelin /// similar to cornifelin	LOC567858 /// LOC568023	79.8	61.68	18.12	3.4	2.24	4.62
Dr.106.1.S1_at	Heat shock protein 47*	*hsp47**	420.36	321.44	98.92	3.25	1.79	4.88
Dr.5586.1.S1_at	Similar to peripheral myelin protein 22 (PMP-22) (CD25 protein) (SR13 myelin protein) (Schwann cell membrane glycoprotein) (SAG); peripheral myelin protein 22†‡	LOC558352; *PMP22*†‡	120.92	92.01	28.91	3.18	1.89	4.58
Dr.1372.1.S1_at	Keratin 18*	*krt18**	282.2	214.1	68.1	3.14	2.19	4.25
Dr.17217.1.S1_at	RAB32, member RAS oncogene family*	*rab32**	248.4	186.94	61.46	3.04	1.84	4.25
Dr.23829.1.A1_at	wu:fc06b08	wu:fc06b08	60.08	45.12	14.96	3.02	1.45	4.67
Dr.636.1.S1_at	zgc:65819; Myoglobin‡†	zgc:65819; *MB*†‡	390.98	292.03	98.95	2.95	1.88	4.03
Dr.20214.1.A1_at	Tubulin, alpha 8 like 3*	*tuba813**	490.37	364.48	125.89	2.9	1.95	4.07
Dr.973.1.S1_at	wu:fb05a01; AHNAK nucleoprotein (desmoyokin)‡*	wu:fb05a01: *AHNAK**‡	259.62	192.53	67.09	2.87	1.71	4.09
Dr.4171.1.A1_at	Phenylalanine hydroxylase*	*pah**	179.59	132.15	47.44	2.79	1.92	3.74
Dr.8594.1.S1_at	zgc:100919	zgc:100919	895.49	653.85	241.64	2.71	1.73	3.84
Dr.23788.1.S1_at	Glutathione S-transferase pi*	*gstp1**	1482.41	1077.38	405.03	2.66	1.83	3.72
Dr.12451.1.S1_at	zgc:73213; Retinal pigment epithelium-specific protein 65kDa*‡	zgc:73213; *RPE65**‡	158.13	114.39	43.73	2.62	1.75	3.51
Dr.17003.1.A1_at	Transcribed locus	—	895.77	647.28	248.48	2.6	1.9	3.39
Dr.12898.1.A1_at	Transcribed locus	—	338.9	243.24	95.65	2.54	1.46	3.65
Dr.3275.1.A1_at	Glycerol-3-phosphate dehydrogenase 1 (soluble), like*	*gpd1l**	130.64	92.29	38.35	2.41	1.48	3.35
Dr.890.1.S1_at	zgc:77517; Keratin 18*‡	zgc:77517; *KRT18**‡	79.18	55.55	23.62	2.35	1.25	3.54
Dr.2211.1.A1_at	Transcribed locus; tumor necrosis factor receptor superfamily, member 10b*‡	—; *TNFRSF10B**‡	252	174.09	77.91	2.23	1.7	2.85
Dr.13861.1.A1_at	Transcribed locus	—	298.84	205.13	93.71	2.19	1.84	2.55

(*continues*)

TABLE 2. (*continued*). Seventy-Eight Overexpressed Genes in the RPE Compared with the Retina at 52 hpf

Probe Set ID	Gene Name	Gene Symbol	Adjusted WRR52 Mean Expression	RPE52 Estimate	WR52 Mean Expression	Fold Change of RPE52/WR52	90% Lower Limit of RPE52/WR52	90% Upper Limit of RPE52/WR52
Dr.14430.1.S1_at	Similar to tumor promoter D52 protein; calcium sensitive phosphoprotein (CSPP28); N8 gene product long isoform (N8L protein) /// similar to prostate and colon associated protein; tumor protein D52*‡	LOC559992 /// LOC563592; *TPD52**‡	123.71	84.49	39.22	2.15	1.65	2.74
Dr.8647.1.A1_at	ADP-ribosylation factor interacting protein 1 (arfaptin 1)*	*arfip1**	191.3	130.56	60.74	2.15	1.35	3.09
Dr.22360.1.A1_at	zgc:85890; Aquaporin 1 (Colton blood group)*‡	zgc:85890; *AQP1**‡	494.6	337.62	156.98	2.15	1.25	3.18
Dr.22408.1.A1_at	wu:fj66d05	wu:fj66d05	216.58	147.62	68.96	2.14	1.4	2.91
Dr.12469.1.S1_at	Arrestin 3, retinal (X-arrestin), like*	*arr3l**	408.3	278.01	130.29	2.13	1.26	3.23
Dr.441.1.S1_at	Procollagen, type IX, alpha 2*	*col9a2**	316.65	215.36	101.29	2.13	1.07	3.36
Dr.9746.4.S1_at	Enolase 3, (beta, muscle)*	*eno3**	285.85	194.11	91.73	2.12	1.47	2.94
Dr.24311.1.S1_at	Nonmetastatic cells 4, protein expressed in*	*nme4**	83.98	56.81	27.17	2.09	1.01	3.18
Dr.481.1.S1_at	Similar to 5-aminoimidazole-4-carboxamide ribonucleotide formyltransferase/IMP cyclohydrolase; 5-Aminoimidazole-4-carboxamide ribonucleotide formyltransferase/IMP cyclohydrolase*‡	LOC555325; *ATIC**‡	1142.71	771.75	370.96	2.08	1.38	3.02
Dr.12080.1.A1_at	— Galactosidase, beta 1-like*‡	— *GLB1L**‡	236.99	159.2	77.79	2.05	1.7	2.41
Dr.25736.1.S1_at	zgc:110591	zgc:110591	285.62	192.02	93.6	2.05	1.16	3.15
Dr.15757.3.A1_at	zgc:100960	zgc:100960	174.78	116.25	58.53	1.99	1.47	2.52
Dr.23928.1.A1_at	wu:fd57e01; Four and a half LIM domains 3*‡	wu:fd57e01; *FHL3**‡	62.93	41.91	21.02	1.99	1.22	2.86
Dr.5586.2.A1_at	Similar to Peripheral myelin protein 22 (PMP-22) (CD25 protein) (SR13 myelin protein) (Schwann cell membrane glycoprotein) (SAG); Peripheral myelin protein 22†‡	LOC558352; PMP22†‡	154.75	101.56	53.19	1.91	1.54	2.32
Dr.4762.2.A1_at	— Transmembrane emp24 protein transport domain containing 3*‡	— *TMED3**‡	446	292.18	153.83	1.9	1.43	2.43
Dr.4129.1.S1_at	Laminin, beta 1*	*lamb1**	95.34	62.19	33.15	1.88	1.49	2.35
Dr.25970.1.A1_at	wu:fj65e07	wu:fj65e07	379.48	246.29	133.19	1.85	1.2	2.53
Dr.18075.3.A1_s_at	zgc:112517 /// similar to mitochondrial ribosomal protein S18-2; Mitochondrial ribosomal protein S18B‡†	zgc:112517 /// LOC573662; *MRPS18B*†‡	947.69	613.61	334.08	1.84	1.48	2.23
Dr.2363.1.S1_at	Transgelin 2* /// similar to transgelin 2 /// similar to transgelin 2	*tagln2** /// LOC565896 /// LOC569306	232.52	150.57	81.95	1.84	1.22	2.5
Dr.2204.1.A1_at	wu:fc15g08	wu:fc15g08	870.22	563.31	306.92	1.84	1.17	2.63

(*continues*)

TABLE 2. (*continued*). Seventy-Eight Overexpressed Genes in the RPE Compared with the Retina at 52 hpf

Probe Set ID	Gene Name	Gene Symbol	Adjusted WRR52 Mean Expression	RPE52 Estimate	WR52 Mean Expression	Fold Change of RPE52/WR52	90% Lower Limit of RPE52/WR52	90% Upper Limit of RPE52/WR52
Dr.20198.2.S1_x_at	Similar to Hsp70 protein; Heat shock cognate 70-kd protein*§	LOC559123; *hsp70**§	154.12	99.08	55.04	1.8	1.45	2.2
Dr.20398.1.A1_a_at	zgc:110081; Acyl-CoA synthetase long-chain family member 1*‡	zgc:110081; *ACSL1**‡	312.68	200.9	111.77	1.8	1.26	2.46
Dr.25185.1.S1_s_at	Hypothetical protein LOC556661 /// similar to Transketolase (TK) /// hypothetical protein LOC559943 /// hypothetical protein LOC561093 /// hypothetical protein LOC561386 /// hypothetical protein LOC563737 /// hypothetical protein LOC563815 /// hypothetical protein LOC567872 /// hypothetical protein LOC568388 /// similar to eukaryotic translation initiation factor 4 gamma, 3 /// hypothetical protein LOC568801 /// hypothetical protein LOC569673 /// hypothetical protein LOC570093 /// similar to MAX dimerization protein 1	LOC556661 /// LOC557518 /// LOC559943 /// LOC561093 /// LOC561386 /// LOC563737 /// LOC563815 /// LOC567872 /// LOC568388 /// LOC568761 /// LOC568801 /// LOC569673 /// LOC570093 /// LOC570102	875.46	562.24	313.22	1.8	1.23	2.46
Dr.1260.1.S1_at	Annexin A2a*	*anxa2a**	65.26	41.87	23.38	1.79	1.27	2.41
Dr.16885.1.A1_at	zgc:110661	zgc:110661	340.44	217.48	122.96	1.77	1.23	2.32
Dr.20198.1.S1_a_at	Heat shock cognate 70-kd protein*	*hsp70**	92.2	58.76	33.44	1.76	1.36	2.18
DrAffx.2.1.S1_at	Runt-related transcription factor 2a	*runx2a**	89.79	57.11	32.68	1.75	1.39	2.14
Dr.20010.10.A1_at	zgc:85677	zgc:85677	520.55	330.78	189.77	1.74	1.21	2.53
Dr.14963.1.A1_at	Similar to C type lectin receptor A /// similar to C type lectin receptor A	LOC564061 /// LOC564448	132.09	83.57	48.52	1.72	1.13	2.31
Dr.23540.1.S1_at	Similar to endoplasmic reticulum lumenal L-amino acid oxidase	LOC556554	78.5	49.42	29.08	1.7	1.02	2.52
Dr.10492.2.A1_at	Alpha-2,8-sialyltransferase ST8Sia I	—	231.81	145.34	86.46	1.68	1.34	2.04
Dr.23827.1.A1_at	wu:fc12a01	wu:fc12a01	1917.29	1196.1	721.19	1.66	1.01	2.33
Dr.1230.1.A1_at	Similar to myoferlin isoform b	LOC564827	84.41	52.23	32.18	1.62	1.1	2.19
Dr.15895.1.S1_a_at	zgc:101624	zgc:101624	67.63	41.84	25.79	1.62	1.06	2.22
Dr.1128.1.S1_at	Carboxypeptidase N, polypeptide 1	*cpn1*†	153.53	94.17	59.36	1.59	1.14	2.11
Dr.18376.1.S1_at	zgc:56538	zgc:56538	135.21	83.04	52.16	1.59	1.13	2.09
Dr.4801.1.S1_at	Phosphoribosylglycinamide formyltransferase	*gart**	245.88	151.03	94.85	1.59	1.12	2.07
Dr.13050.1.S1_at	zgc:110459; Pleckstrin homology-like domain, family A, member 2‡†	zgc:110459; *PHLDA2*†‡	87.33	53.2	34.13	1.56	1.11	2.04

(*continues*)

TABLE 2. (*continued*). Seventy-Eight Overexpressed Genes in the RPE Compared with the Retina at 52 hpf

Probe Set ID	Gene Name	Gene Symbol	Adjusted WRR52 Mean Expression	RPE52 Estimate	WR52 Mean Expression	Fold Change of RPE52/WR52	90% Lower Limit of RPE52/WR52	90% Upper Limit of RPE52/WR52
Dr.13799.1.S1_x_at	Hypothetical protein LOC407696	LOC407696	117.33	70.59	46.75	1.51	1.11	1.94
Dr.3459.1.S1_at	Cd63 antigen	*cd163**	1591.64	956.47	635.17	1.51	1.02	2.02
Dr.15412.2.S1_a_at	zgc:101720; Tumor suppressing subtransferable candidate 1‡†	zgc:101720; *TSSC1*†‡	509.91	306.03	203.88	1.5	1.1	2
Dr.1361.1.S1_at	— Keratin 13†‡	— *KRT13*†‡	96.98	57.71	39.26	1.47	1.16	1.79
Dr.2194.1.A1_at	Similar to LL5 beta protein	LOC560668	42.77	25.4	17.37	1.46	1.26	1.67
Dr.9478.4.S1_a_at	Myeloid-specific peroxidase†	*mpx*†	153.11	90.75	62.36	1.46	1.02	1.91
Dr.15096.1.A1_at	zgc:110702	zgc:110702	296.2	170.39	125.81	1.35	1.03	1.67
Dr.21055.1.S1_at	zgc:56197; RAD9 homolog A (S. pombe)†‡	zgc:56197; *RAD9A*†‡	185.41	104.61	80.81	1.29	1.15	1.44

* These probesets have been experimentally validated to be RPE-related transcripts.

† There are no experimental data to date that show the expression of these genes in the RPE.

‡ Symbol and name of the human homologue obtained from the Ensembl database (http://www.ensembl.org/).

§ *hsp70* is not annotated in the Affymetrix annotation file used in this study, but the probe set is annotated as zebrafish *hsp70* in the Ensembl database (version Zv5, May 2005).

In conclusion, the present study has demonstrated the feasibility of studying differential gene expression of the developing RPE in zebrafish in vivo. Together with the retinal expression profiling methodology, they have opened up the possibility of performing a time-series study on early RPE and retinal development in parallel using the zebrafish model, and obtaining system-level data for understanding how the gene networks in retina and RPE operate together to build a functioning retina.

Acknowledgments

The authors thank Jennifer Couget and ShuFen Meng for excellent assistance with the Affymetrix GeneChip experiments.

References

1. Strauss O. The retinal pigment epithelium in visual function. *Physiol Rev*. 2005;85:845–881.
2. Dowling JE. Retina. In: Ramachandran VS, ed. *Encyclopedia of the Human Brain.* San Diego, CA: Academic Press; 2002:217–235.
3. Jablonski MM, Tombran-Tink J, Mrazek DA, Iannaccone A. Pigment epithelium-derived factor supports normal development of photoreceptor neurons and opsin expression after retinal pigment epithelium removal. *J Neurosci*. 2000;20:7149–7157.
4. Stenkamp DL, Frey RA, Prabhudesai SN, Raymond PA. Function for Hedgehog genes in zebrafish retinal development. *Dev Biol*. 2000; 220:238–252.
5. Phelan JK, Bok D. A brief review of retinitis pigmentosa and the identified retinitis pigmentosa genes. *Mol Vis*. 2000;6:116–124.
6. Green WR. Histopathology of age-related macular degeneration. *Mol Vis*. 1999;5:27.
7. Honda S, Farboud B, Hjelmeland LM, Handa JT. Induction of an aging mRNA retinal pigment epithelial cell phenotype by matrix-containing advanced glycation end products in vitro. *Invest Ophthalmol Vis Sci*. 2001;42:2419–2425.
8. Singh S, Zheng JJ, Peiper SC, McLaughlin BJ. Gene expression profile of ARPE-19 during repair of the monolayer. *Graefes Arch Clin Exp Ophthalmol*. 2001;239:946–951.
9. Buraczynska M, Mears AJ, Zareparsi S, et al. Gene expression profile of native human retinal pigment epithelium. *Invest Ophthalmol Vis Sci*. 2002;43:603–607.
10. Weigel AL, Handa JT, Hjelmeland LM. Microarray analysis of H_2O_2-, HNE-, or tBH-treated ARPE-19 cells. *Free Radic Biol Med*. 2002; 33:1419–1432.
11. Rogojina AT, Orr WE, Song BK, Geisert EE, Jr. Comparing the use of Affymetrix to spotted oligonucleotide microarrays using two retinal pigment epithelium cell lines. *Mol Vis*. 2003;9:482–496.
12. Tian J, Ishibashi K, Handa JT. The expression of native and cultured RPE grown on different matrices. *Physiol Genomics*. 2004; 17:170–182.
13. Chowers I, Kim Y, Farkas RH, et al. Changes in retinal pigment epithelial gene expression induced by rod outer segment uptake. *Invest Ophthalmol Vis Sci*. 2004;45:2098–2106.
14. Sharma RK, Orr WE, Schmitt AD, Johnson DA. A functional profile of gene expression in ARPE-19 cells. *BMC Ophthalmol*. 2005;5:25.
15. Tian J, Ishibashi K, Reiser K, et al. Advanced glycation endproduct-induced aging of the retinal pigment epithelium and choroid: a comprehensive transcriptional response. *Proc Natl Acad Sci USA*. 2005;102:11846–11851.
16. Yu X, Tang Y, Li F, et al. Protection against hydrogen peroxide-induced cell death in cultured human retinal pigment epithelial cells by 17beta-estradiol: a differential gene expression profile. *Mech Ageing Dev*. 2005;126:1135–1145.
17. Cai H, Del Priore LV. Bruch membrane aging alters the gene expression profile of human retinal pigment epithelium. *Curr Eye Res*. 2006;31:181–189.
18. Cai H, Del Priore LV. Gene expression profile of cultured adult compared with immortalized human RPE. *Mol Vis*. 2006;12:1–14.
19. Sharon D, Blackshaw S, Cepko CL, Dryja TP. Profile of the genes expressed in the human peripheral retina, macula, and retinal pigment epithelium determined through serial analysis of gene expression (SAGE). *Proc Natl Acad Sci USA*. 2002;99:315–320.
20. Wiechmann AF. Regulation of gene expression by melatonin: a microarray survey of the rat retina. *J Pineal Res*. 2002;33:178–185.
21. Wistow G, Bernstein SL, Wyatt MK, et al. Expressed sequence tag analysis of human RPE/choroid for the NEIBank Project: over 6000 non-redundant transcripts, novel genes and splice variants. *Mol Vis*. 2002;8:205–220.
22. Dufour EM, Nandrot E, Marchant D, et al. Identification of novel genes and altered signaling pathways in the retinal pigment epithelium during the Royal College of Surgeons rat retinal degeneration. *Neurobiol Dis*. 2003;14:166–180.
23. Ida H, Boylan SA, Weigel AL, Hjelmeland LM. Age-related changes in the transcriptional profile of mouse RPE/choroid. *Physiol Genomics*. 2003;15:258–262.

24. Wilson AS, Hobbs BG, Shen WY, et al. Argon laser photocoagulation-induced modification of gene expression in the retina. *Invest Ophthalmol Vis Sci*. 2003;44:1426–1434.
25. Kobashi-Hashida M, Ohguro N, Tsujikawa M, et al. Micro serial analysis of gene expression in normal human choroid and retinal pigment epithelial transcriptomes. *Jpn J Ophthalmol*. 2005;49:15–22.
26. Tian J, Ishibashi K, Honda S, Boylan SA, Hjelmeland LM, Handa JT. The expression of native and cultured human retinal pigment epithelial cells grown in different culture conditions. *Br J Ophthalmol*. 2005;89:1510–1517.
27. Soukas A, Socci ND, Saatkamp BD, Novelli S, Friedman JM. Distinct transcriptional profiles of adipogenesis in vivo and in vitro. *J Biol Chem*. 2001;276:34167–34174.
28. Boess F, Kamber M, Romer S, et al. Gene expression in two hepatic cell lines, cultured primary hepatocytes, and liver slices compared with the in vivo liver gene expression in rats: possible implications for toxicogenomics use of in vitro systems. *Toxicol Sci*. 2003;73:386–402.
29. Sandberg R, Ernberg I. The molecular portrait of in vitro growth by meta-analysis of gene-expression profiles. *Genome Biol*. 2005;6:R65.
30. Leung YF, Dowling JE. Gene expression profiling of zebrafish embryonic retina. *Zebrafish*. 2005;2:269–283.
31. Westerfield M. *The Zebrafish Book: a Guide for the Laboratory Use of Zebrafish (Danio rerio)*. 4th ed. Eugene, OR: University of Oregon Press; 2000.
32. Irizarry RA, Hobbs B, Collin F, et al. Exploration, normalization, and summaries of high density oligonucleotide array probe level data. *Biostatistics*. 2003;4:249–264.
33. Serfling RJ. *Approximation Theorems of Mathematical Statistics*. New York: John Wiley & Sons; 1980:xiv,371.
34. Li C, Hung Wong W. Model-based analysis of oligonucleotide arrays: model validation, design issues and standard error application. *Genome Biol.* 2001;2:RESEARCH0032.
35. Cox DR, Hinkley DV. *Theoretical Statistics*. London: Chapman and Hall; 1974.
36. Schmitt EA, Dowling JE. Comparison of topographical patterns of ganglion and photoreceptor cell differentiation in the retina of the zebrafish, Danio rerio. *J Comp Neurol*. 1996;371:222–234.
37. Dowling JE, Sidman RL. Inherited retinal dystrophy in the rat. *J Cell Biol*. 1962;14:73–109.
38. LaVail MM. Kinetics of rod outer segment renewal in the developing mouse retina. *J Cell Biol*. 1973;58:650–661.
39. Kelsh RN, Schmid B, Eisen JS. Genetic analysis of melanophore development in zebrafish embryos. *Dev Biol*. 2000;225:277–293.
40. Parichy DM, Ransom DG, Paw B, Zon LI, Johnson SL. An orthologue of the kit-related gene fms is required for development of neural crest-derived xanthophores and a subpopulation of adult melanocytes in the zebrafish, Danio rerio. *Development*. 2000;127:3031–3044.
41. Knight RD, Nair S, Nelson SS, et al. lockjaw encodes a zebrafish tfap2a required for early neural crest development. *Development*. 2003;130:5755–5768.
42. Arduini BL, Henion PD. Melanophore sublineage-specific requirement for zebrafish touchtone during neural crest development. *Mech Dev*. 2004;121:1353–1364.
43. Candy J, Collet C. Two tyrosine hydroxylase genes in teleosts. *Biochim Biophys Acta*. 2005;1727:35–44.
44. Thisse B, Pflumio S, Furthauer M, et al. *Expression of the Zebrafish Genome during Embryogenesis* (*NIH R01 RR15402*). Eugene, OR: University of Oregon, ZFIN (Zebrafish Information Network) Direct Data Submission; 2001.
45. Thisse B, Thisse C. Fast Release Clones: *A High Throughput Expression Analysis*. Eugene, OR: University of Oregon, ZFIN Direct Data Submission; 2004.
46. Jin M, Li S, Moghrabi WN, Sun H, Travis GH. Rpe65 is the retinoid isomerase in bovine retinal pigment epithelium. *Cell*. 2005;122:449–459.
47. Chen P, Lee TD, Fong HK. Interaction of 11-cis-retinol dehydrogenase with the chromophore of retinal g protein-coupled receptor opsin. *J Biol Chem*. 2001;276:21098–21104.
48. Stamer WD, Bok D, Hu J, Jaffe GJ, McKay BS. Aquaporin-1 channels in human retinal pigment epithelium: role in transepithelial water movement. *Invest Ophthalmol Vis Sci*. 2003;44:2803–2808.
49. Gross JM, Perkins BD, Amsterdam A, et al. Identification of zebrafish insertional mutants with defects in visual system development and function. *Genetics*. 2005;170:245–261.
50. Amsterdam A, Nissen RM, Sun Z, Swindell EC, Farrington S, Hopkins N. Identification of 315 genes essential for early zebrafish development. *Proc Natl Acad Sci USA*. 2004;101:12792–12797.
51. Klimanskaya I, Hipp J, Rezai KA, West M, Atala A, Lanza R. Derivation and comparative assessment of retinal pigment epithelium from human embryonic stem cells using transcriptomics. *Cloning Stem Cells*. 2004;6:217–245.
52. Zhao Q, Eberspaecher H, Lefebvre V, De Crombrugghe B. Parallel expression of Sox9 and Col2a1 in cells undergoing chondrogenesis. *Dev Dyn*. 1997;209:377–386.
53. Bonilha VL, Bhattacharya SK, West KA, et al. Proteomic characterization of isolated retinal pigment epithelium microvilli. *Mol Cell Proteomics*. 2004;3:1119–1127.
54. Nordgaard CL, Berg KM, Kapphahn RJ, et al. Proteomics of the retinal pigment epithelium reveals altered protein expression at progressive stages of age-related macular degeneration. *Invest Ophthalmol Vis Sci*. 2006;47:815–822.
55. Liu Q, Babb SG, Novince ZM, Doedens AL, Marrs J, Raymond PA. Differential expression of cadherin-2 and cadherin-4 in the developing and adult zebrafish visual system. *Vis Neurosci*. 2001;18:923–933.
56. Fashena D, Westerfield M. Secondary motoneuron axons localize DM-GRASP on their fasciculated segments. *J Comp Neurol*. 1999;406:415–424.
57. Kay JN, Finger-Baier KC, Roeser T, Staub W, Baier H. Retinal ganglion cell genesis requires lakritz, a zebrafish atonal homolog. *Neuron*. 2001;30:725–736.
58. Easter SS Jr, Nicola GN. The development of vision in the zebrafish (Danio rerio). *Dev Biol*. 1996;180:646–663.
59. Easter SS Jr, Nicola GN. The development of eye movements in the zebrafish (Danio rerio). *Dev Psychobiol*. 1997;31:267–276.
60. Hu M, Easter SS. Retinal neurogenesis: the formation of the initial central patch of postmitotic cells. *Dev Biol*. 1999;207:309–321.
61. Neumann CJ. Pattern formation in the zebrafish retina. *Semin Cell Dev Biol*. 2001;12:485–490.